

基于海流观测器对欠驱动水下机器人进行三维路径跟随

杨 莹^{1,2}, 夏国清^{1†}, 赵为光²

(1. 哈尔滨工程大学 自动化学院, 黑龙江 哈尔滨 150001; 2. 黑龙江科技大学 电气与控制工程学院, 黑龙江 哈尔滨 150022)

摘要: 对模型参数未知的欠驱动水下机器人, 本文设计了海流中三维路径跟随控制器。该方法在无旋流的前提下, 利用海流的运动方程, 结合三维视线导航法和反步法, 设计了控制器。通过死区方法估计模型参数, 克服了参数漂移问题; 针对海流未知情况, 设计了海流观测器。最后通过Lyapunov稳定性理论证明了跟踪误差是收敛的, 仿真实验验证了该控制方法的有效性。

关键词: 自主水下机器人; 路径跟随; 死区方法; 海流观测器

中图分类号: TP273 文献标识码: A

Path-following in 3D for underactuated autonomous underwater vehicle based on ocean-current observer

YANG Ying^{1,2}, XIA Guo-qing^{1†}, ZHAO Wei-guang²

(1. College of Automation, Harbin Engineering University, Harbin Heilongjiang 150001, China;
2. College of Electric & Information Engineering, Heilongjiang Institute of Science & Technology, Harbin Heilongjiang 150022, China)

Abstract: A path-following controller in 3D is developed for an underactuated autonomous underwater vehicle with unknown physical parameters in the presence of ocean-current. Assuming the current is irrotational, we design the controller based on the motion equations of the ocean currents by combining with the line of sight (LOS) guidance algorithm and the backstepping technique. The dead-zone methods are used to estimate the unknown parameters to avoid the parameter drift. The current observer is used to estimate unknown ocean-current velocities. Finally, the stability analysis is carried out by using Lyapunov stability theory. Numerical simulations show the effectiveness of the proposed controller.

Key words: autonomous underwater vehicles; path following; dead-zone method; ocean-current observer

1 引言(Introduction)

随着科技的迅速发展, 水下机器人在深海资源勘探开发、海洋水文观测、海洋测量等民用领域及军事领域得到广泛关注。目前, 大多数水下航行器都是欠驱动系统, 其具有重量轻、成本低、能耗低等优点, 然而欠驱动系统的本质特性以及控制方法研究, 涉及到泛函、群论、微分几何、李代数等抽象的数学工具, 使控制问题较为复杂。因此, 欠驱动水下机器人的控制方法研究具有重要的实际意义^[1-3]。

欠驱动自主水下航行器(autonomous underwater vehicles, AUV)控制的主要困难在于系统的被控自由度比控制输入数量多。如果将用于全驱动或过驱动的经典控制方法直接用于欠驱动系统, 会导致被控系统性能降低或不能达到控制目标。目前, 对于欠驱动系统常用的控制方法有反步法、级联理论、Lyapunov理论等^[4], 文献[5]提出了输出反馈控制器同时解决了全局渐近稳定和欠驱动全方向智能航行器(omni-directional intelligent navigator, ODIN)的跟踪, 控制方法采用Lyapunov直接法和反步法。文献[6]针对未知海流和模型参数不确定情况下欠驱动AUV的动力定位和路径点跟踪, 采用Lyapunov理论和反步法将运动学控制器扩展到动态模型。文献[7]基于Lyapunov理论和反步法提出了欠驱动AUV的路径跟随方法, 该方法克服了严格的初始条件约束, 使路径跟踪误差收敛到零。

前面提到的文献都是欠驱动AUV的平面控制, 如果将这些方法直接应用到三维空间中, 由于只有轴向推力、俯仰力矩和偏航力矩, 使控制问题遇到很大挑战。文献[8]基于导航算法提出了三维空间欠驱动AUV非线性控制器, 但该文未考虑海流影响。文献[9]模型中考虑了海流速度, 并设计了海流观测器, 但要求三维控制器中的模型参数已知。文献[10]设计了三维空间欠驱动AUV的输出反馈控制器, 同样要求模型参数已知。

本文采用文献[8]提出的三维视线(line of sight,

收稿日期: 2012-12-05; 收修改稿日期: 2013-03-28.

†通信作者。E-mail: xiaguoqing@hrbeu.edu.cn.

基金项目: 国家自然科学基金资助项目(50979017).

LOS)导航算法, 考虑存在海流干扰条件下, 模型参数未知的欠驱动AUV三维路径跟随问题。首先, 利用三维空间的LOS导航算法, 设计期望俯仰角和偏航角; 进而利用反步法得到轴向推力、俯仰力矩及偏航力矩; 并通过死区方法估计控制输入中的未知模型参数, 以克服参数漂移问题; 对未知的海流速度设计观测器; 最后, 通过Lyapunov稳定性理论及仿真实验证明了该控制方法能使跟踪误差一致有界。

2 包含海流因素的欠驱动 AUV 模型(Underactuated AUV model considering ocean-current)

考虑海流对AUV的影响, 欠驱动AUV六自由度模型如下^[11]:

$$\dot{\eta} = J(\Theta)\nu, \quad (1)$$

$$M\dot{\nu} + C_{RB}(\nu)\nu + C_A(\nu_r)\nu_r +$$

$$D(\nu_r)\nu_r + g(\eta) = \tau, \quad (2)$$

其中 $J(\Theta) = \begin{bmatrix} R(\Theta) & \mathbf{0}_{3 \times 3} \\ \mathbf{0}_{3 \times 3} & T(\Theta) \end{bmatrix}$, 为简化符号, $c \cdot = \cos(\cdot)$, $s \cdot = \sin(\cdot)$, $t \cdot = \tan(\cdot)$,

$$R(\Theta) = \begin{bmatrix} c\psi c\theta - s\psi c\varphi + c\psi s\theta s\varphi & s\psi s\varphi + c\psi c\varphi s\theta & \\ s\psi c\theta & c\psi c\varphi + s\varphi s\theta s\psi & -c\psi s\varphi + s\theta s\psi c\varphi \\ -s\theta & c\theta s\varphi & c\theta c\varphi \end{bmatrix},$$

$$T(\Theta) = \begin{bmatrix} 1 & s\varphi t\theta & c\varphi t\theta \\ 0 & c\varphi & -s\varphi \\ 0 & s\varphi/c\theta & c\varphi/c\theta \end{bmatrix},$$

其中: $\eta = (x, y, z, \varphi, \theta, \psi)^T$ 是惯性坐标系下的位置和角度; $\nu = (\nu_1, \nu_2)^T = (u, v, w, p, q, r)^T$ 表示体坐标系下的速度; $\Theta = (\varphi, \theta, \psi)^T$, $\tau = (\tau_u, 0, 0, 0, \tau_q, \tau_r)^T$, $\nu_r = \nu - V_c$, $V_c = (u_c, v_c, w_c, 0_{1 \times 3})^T \in \mathbb{R}^6$ 表示体坐标系下海流速度。且满足

$$\begin{cases} M = M^T > 0, \dot{M} = 0, \\ C_{RB}(\nu) = -C_{RB}^T(\nu), x^T C_{RB}(\nu)x = 0, \\ C_A(\nu_r) = -C_A^T(\nu_r), x^T C_A(\nu_r)x = 0, \\ x^T D(\nu)x > 0, \forall \nu \in \mathbb{R}^6 \setminus \{0\}, \dot{V}_c = 0, \end{cases} \quad (3)$$

本文的控制目标是在存在未知的常值海流干扰和模型参数不确定情况下, 对轴向推力、俯仰力矩及偏航力矩设计反馈控制律使AUV位置(x, y, z)精确跟踪期望轨迹(x_d, y_d, z_d), 且所有闭环系统信号是最终有界的。

3 非线性控制器设计(Nonlinear controller design)

图1为欠驱动AUV非线性控制原理图。控制器由非线性控制器、海流观测器、参数估计器、滤波器组成。

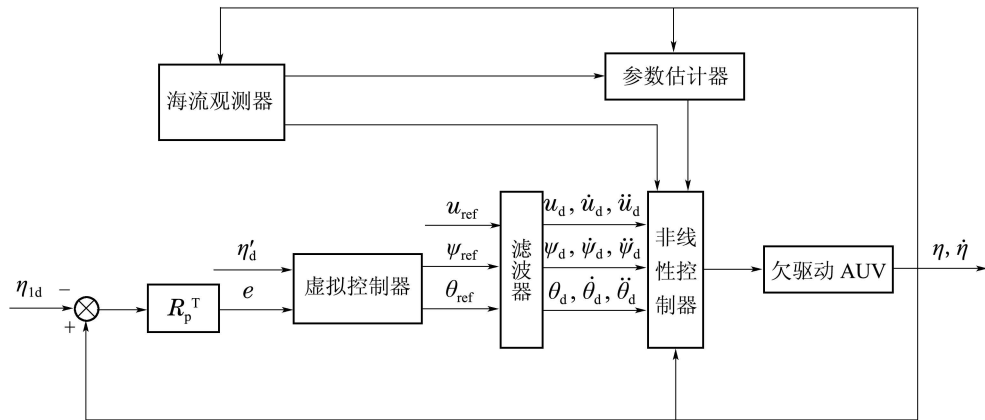


图1 欠驱动AUV非线性控制原理图

Fig. 1 Principle scheme of nonlinear control of underactuated AUV

3.1 控制器设计(Controller design)

定义跟踪误差

$$e = (e_1, e_2, e_3)^T = R_p^T(P - P_d), \quad (4)$$

其中: $P = (x(t), y(t), z(t))^T \in \mathbb{R}^3$ 表示AUV的实际位置, $P_d = (x_d(s), y_d(s), z_d(s))^T \in \mathbb{R}^3$ 为期望路径,

$$R_p = \begin{bmatrix} \cos \chi_p \cos v_p & -\sin \chi_p \cos \chi_p \sin v_p & \\ \sin \chi_p \cos v_p & \cos \chi_p & \sin \chi_p \sin v_p \\ -\sin v_p & 0 & \cos v_p \end{bmatrix},$$

$$\chi_p(s) = \arctan \frac{y'_d(s)}{x'_d(s)},$$

$$v_p(s) = \arctan \frac{-z'_d(s)}{\sqrt{x'^2_d(s) + y'^2_d(s)}},$$

以下符号对应含义:

$$x'_d(s) = \frac{dx_d}{ds}, y'_d(s) = \frac{dy_d}{ds}, z'_d(s) = \frac{dz_d}{ds},$$

$$\dot{x}_d(s) = \frac{\partial x_d}{\partial s} \dot{s}, \dot{y}_d(s) = \frac{\partial y_d}{\partial s} \dot{s}, \dot{z}_d(s) = \frac{\partial z_d}{\partial s} \dot{s},$$

其中 s 为期望路径算子。

定义 $\{X_p, Y_p, Z_p\}$ 为期望路径坐标系, 令 v_R 表示 $\{X_p, Y_p\}$ 平面到AUV实际速度 \dot{P} 的角度, χ_R 表示坐

标轴 X_p 到 \dot{P} 夹角在 $\{X_p, Y_p\}$ 平面投影.

则位置误差动态为

$$\begin{cases} \dot{e}_1 = e_2 \dot{\chi}_p \cos v_p - e_3 \dot{v}_p + U \cos \chi_R \cos v_R - U_p, \\ \dot{e}_2 = -e_1 \dot{\chi}_p \cos v_p - e_3 \dot{\chi}_p \sin v_p + U \sin \chi_R \cos v_R, \\ \dot{e}_3 = e_1 \dot{v}_p + e_2 \dot{\chi}_p \sin v_p - U \sin v_R, \end{cases} \quad (5)$$

其中 $U_p = \sqrt{\dot{x}_d^2 + \dot{y}_d^2 + \dot{z}_d^2}$.

$$v_d = \arcsin(\sin v_p \cos v_R \cos \chi_R + \cos v_p \sin v_R), \quad (9)$$

$$\chi_d = \arctan\left(\frac{\cos \chi_p \sin \chi_R \cos v_R - \sin v_p \sin v_R \sin \chi_p + \sin \chi_p \cos \chi_R \cos v_p \cos v_R}{-\sin \chi_p \sin \chi_R \cos v_R - \sin v_p \sin v_R \cos \chi_p + \cos \chi_p \cos \chi_R \cos v_p \cos v_R}\right). \quad (10)$$

可知期望俯仰角和偏航角为

$$\theta_{ref} = v_d - \arctan \frac{-w}{\sqrt{u^2 + v^2}}, \quad (11)$$

$$\psi_{ref} = \chi_d - \arctan \frac{v}{u}. \quad (12)$$

设 u_d, θ_d, ψ_d 为 $u_{ref}, \theta_{ref}, \psi_{ref}$ 滤波后的期望值, 其中 u_{ref} 为期望纵向速度, 下面设计实际控制输入轴向推力 τ_u 、俯仰力矩 τ_q 、及偏航力矩 τ_r .

首先定义

$$Z_1 = [z_{11} \ z_{12}]^T = [\theta - \theta_d \ \psi - \psi_d]^T, \quad (13)$$

$$\begin{aligned} Z_2 &= \nu - \alpha = [u - \alpha_1 \ v - \alpha_2 \ w - \alpha_3 \\ &\quad p - \alpha_4 \ q - \alpha_5 \ r - \alpha_6]^T. \end{aligned} \quad (14)$$

虚拟输入量设计为

$$\alpha_1 = u_d, \quad (15)$$

$$\alpha_5 = \cos \varphi (\dot{\theta}_d - z_{11}) + \sin \varphi \cos \theta (\dot{\psi}_d - z_{12}), \quad (16)$$

$$\begin{aligned} \alpha_6 &= -\sin \varphi (\dot{\theta}_d - z_{11}) + \cos \varphi \cos \theta (\dot{\psi}_d - z_{12}). \\ (17) \end{aligned}$$

对式(13)两边求一阶导数, 得

$$\dot{Z}_1 = [\dot{z}_{11} \ \dot{z}_{12}]^T = [\dot{\theta} - \dot{\theta}_d \ \dot{\psi} - \dot{\psi}_d]^T, \quad (18)$$

$$\begin{aligned} \dot{Z}_1 &= T_1[q \ r]^T - [\dot{\theta}_d \ \dot{\psi}_d]^T = \\ &\quad T_1 H(Z_2 + \alpha) - [\dot{\theta}_d \ \dot{\psi}_d]^T, \end{aligned} \quad (19)$$

其中: $T_1(\Theta) = \begin{bmatrix} c\varphi & -s\varphi \\ s\varphi & c\varphi \\ c\theta & c\theta \end{bmatrix}$, $H = \begin{bmatrix} 0 & 0 & 0 & 1 & 0 \\ 0 & 0 & 0 & 0 & 1 \end{bmatrix}$.

结合式(16)–(17)(19), 整理得

$$\dot{Z}_1 = -Z_1 + T_1 H Z_2. \quad (20)$$

对式(14)两边求一阶导数, 并结合AUV模型(2)的动力学方程, 整理得

$$\begin{aligned} M \dot{Z}_2 &= M(\dot{\nu} - \dot{\alpha}) = \\ &\quad \tau - C_{RB}(\nu)(Z_2 + \alpha) - C_A(\nu_r)(Z_2 + \alpha - \\ &\quad V_c) - D(\nu_r)(Z_2 + \alpha - V_c) - g(\eta) - M \dot{\alpha} = \\ &\quad \tau - (C_{RB}(\nu) + C_A(\nu_r) + D(\nu_r))Z_2 - \end{aligned}$$

首先根据三维LOS导航算法得^[8]:

$$\dot{s} = \frac{U \cos \chi_R \cos v_R + \delta_1 e_1}{\sqrt{x_d'^2 + y_d'^2 + z_d'^2}}, \quad (6)$$

$$\chi_R = \arctan -\frac{e_2}{\Delta_1}, \quad (7)$$

$$v_R = \arctan \frac{e_3}{\Delta_2}, \quad (8)$$

其中: $U = \sqrt{\dot{x}^2 + \dot{y}^2 + \dot{z}^2}$, $\Delta_1 > 0$, $\Delta_2 = \delta_2 \sqrt{e_2^2 + \Delta_1^2} > 0$, $\delta_1 > 0$, $\delta_2 > 0$ 为设计参数;

$$(C_{RB}(\nu) + C_A(\nu_r) + D(\nu_r))\alpha + (C_A(\nu_r) +$$

$$D(\nu_r))V_c - g(\eta) - M \dot{\alpha}. \quad (21)$$

设计实际控制输入为

$$\begin{cases} \tau_u = -k_{21} z_{21} + (m - X_{\dot{u}})\dot{\alpha}_1 + m w \alpha_5 - m v \alpha_6 - \\ Z_{\dot{w}} w_r \alpha_5 + Y_{\dot{v}} v_r \alpha_6 + (X_u + X_{u|u|}|u_r|)\alpha_1 - \\ (X_u + X_{u|u|}|u_r|)u_c, \\ \tau_q = -k_{25} z_{25} + g(5) - z_{11} \cos \varphi - \\ z_{12} \sin \varphi \cos \theta + (I_y - M_{\dot{q}})\dot{\alpha}_5 - m w \alpha_1 + \\ m u \alpha_3 - I_z r \alpha_4 + I_x p \alpha_6 + Z_{\dot{w}} w_r \alpha_1 - \\ X_{\dot{u}} u_r \alpha_3 + N_{\dot{r}} r \alpha_4 - K_{\dot{p}} p \alpha_6 - Z_{\dot{w}} w_r u_c + \\ X_{\dot{u}} u_r w_c + (M_q + M_{q|q|}|q|)\alpha_5, \\ \tau_r = -k_{26} z_{26} + z_{11} \sin \varphi - z_{12} \cos \varphi \cos \theta + \\ (I_z - N_{\dot{r}})\dot{\alpha}_6 + m v \alpha_1 - m u \alpha_2 + I_y q \alpha_4 - \\ I_x p \alpha_5 - Y_{\dot{v}} v_r \alpha_1 + X_{\dot{u}} u_r \alpha_2 - M_{\dot{q}} q \alpha_4 + \\ K_{\dot{p}} p \alpha_5 + Y_{\dot{v}} v_r u_c - X_{\dot{u}} u_r v_c + \\ (N_r + N_{r|r|}|r|)\alpha_6, \end{cases} \quad (22)$$

则

$$\begin{cases} (m - Y_{\dot{v}})\dot{\alpha}_2 = m w \alpha_4 - m u \alpha_6 - Z_{\dot{w}} w_r \alpha_4 + \\ X_{\dot{u}} u_r \alpha_6 - (Y_v + Y_{v|v|}|v_r|)\alpha_2 + \\ (Y_v + Y_{v|v|}|v_r|)v_c + k_{22} z_{22}, \\ (m - Z_{\dot{w}})\dot{\alpha}_3 = -m v \alpha_4 + m u \alpha_5 + Y_{\dot{v}} v_r \alpha_4 - \\ X_{\dot{u}} u_r \alpha_5 - (Z_w + Z_{w|w|}|w_r|)\alpha_3 + \\ (Z_w + Z_{w|w|}|w_r|)w_c + k_{23} z_{23}, \\ (I_x - K_{\dot{p}})\dot{\alpha}_4 = -m w \alpha_2 + m v \alpha_3 - I_z r \alpha_5 + \\ I_y q \alpha_6 + Z_{\dot{w}} w_r \alpha_2 - Y_{\dot{v}} v_r \alpha_3 + \\ N_{\dot{r}} r \alpha_5 - M_{\dot{q}} q \alpha_6 - Z_w w_r v_c + \\ Y_{\dot{v}} v_r v_c - (K_p + K_{p|p|}|p|)\alpha_4 - \\ g(4) + k_{24} z_{24}, \end{cases} \quad (23)$$

其中: $k_{21}, k_{22}, k_{23}, k_{24}, k_{25}, k_{26}$ 为控制参数; $g(4)$,

$g(5)$ 分别为 $g(\eta)$ 的第4和第5个元素.

3.2 参数估计律设计(Parameter estimation law design)

前面控制器设计都是在假定AUV模型参数精确已知的前提下, 实际中这个假设难以实现. 下面将控制器式(22)进一步扩展保证其当模型参数不确定时的鲁棒性.

令:

$$\left\{ \begin{array}{l} \Theta_1 = ((m - X_{\dot{u}}), m, Z_{\dot{w}}, Y_{\dot{v}}, X_u, X_{u|u})^T, \\ \Theta_2 = ((I_y - M_{\dot{q}}), m, (N_{\dot{r}} - I_z), (I_x - K_{\dot{p}}), Z_{\dot{w}}, \\ \quad X_{\dot{u}}, M_q, M_{q|q})^T, \\ \Theta_3 = ((I_z - N_r), m, (I_y - M_{\dot{q}}), (K_{\dot{p}} - I_x), Y_{\dot{v}}, \\ \quad X_{\dot{u}}, N_r, N_{r|r})^T, \\ \boldsymbol{w}_1(\cdot) = (\dot{\alpha}_1, w\alpha_5 - v\alpha_6, -w_r\alpha_5, v_r\alpha_6, (\alpha_1 - \\ \quad u_c), |u_r|(\alpha_1 - u_c))^T, \\ \boldsymbol{w}_2(\cdot) = (\dot{\alpha}_5, u\alpha_3 - w\alpha_1, r\alpha_4, p\alpha_6, w_r(\alpha_1 - \\ \quad u_c), u_r(w_c - \alpha_3), \alpha_5, |q|\alpha_5)^T, \\ \boldsymbol{w}_3(\cdot) = (\dot{\alpha}_6, (v\alpha_1 - u\alpha_2), q\alpha_4, p\alpha_5, v_r(u_c - \\ \quad \alpha_1), u_r\alpha_2 - v_c, \alpha_6, |r|\alpha_6)^T. \end{array} \right. \quad (24)$$

为避免参数漂移, 采用死区方法的参数估计律^[12], 即当误差很小时关闭自适应机制. 令: $\tilde{\Theta}_i = \hat{\Theta}_i - \Theta_i$,

$$\left\{ \begin{array}{l} \dot{\tilde{\Theta}}_{1j} = \begin{cases} -\gamma_{1j}z_{21}\boldsymbol{w}_{1j}, & |z_{21}| > \Delta \\ 0, & |z_{21}| < \Delta \end{cases}, \quad 1 \leq j \leq 6, \\ \dot{\tilde{\Theta}}_{2j} = \begin{cases} -\gamma_{2j}z_{25}\boldsymbol{w}_{2j}, & |z_{25}| > \Delta \\ 0, & |z_{25}| < \Delta \end{cases}, \quad 1 \leq j \leq 8, \\ \dot{\tilde{\Theta}}_{3j} = \begin{cases} -\gamma_{3j}z_{26}\boldsymbol{w}_{3j}, & |z_{26}| > \Delta \\ 0, & |z_{26}| < \Delta \end{cases}, \quad 1 \leq j \leq 8, \end{array} \right. \quad (25)$$

其中: Δ 是死区的大小, $\gamma_{ij} > 0$, $1 \leq i \leq 3$. 则自适应控制器为

$$\left\{ \begin{array}{l} \tau_u = -k_{21}z_{21} + \hat{\Theta}_1^T \boldsymbol{w}_1, \\ \tau_q = -z_{11}\cos\varphi - z_{12}\sin\varphi\cos\theta - \\ \quad k_{25}z_{25} + g(5) + \hat{\Theta}_2^T \boldsymbol{w}_2, \\ \tau_r = -k_{26}z_{26} + z_{11}\sin\varphi - \\ \quad z_{12}\cos\varphi\cos\theta + \hat{\Theta}_3^T \boldsymbol{w}_3. \end{array} \right. \quad (26)$$

3.3 滤波器设计(Filter design)

为获得光滑、连续的参考路径高阶导数, 定义如下滤波器^[10]:

$$\left\{ \begin{array}{l} \ddot{u}_d = -(2\zeta_1\omega_1 + \zeta_2|\dot{u}_d|)\dot{u}_d - \omega_1^2(u_d - u_{ref}), \\ \dot{\theta}_d = q_d, \\ \dot{\psi}_d = \frac{1}{\cos\theta}r_d, \\ \ddot{q}_d = -2(\zeta_3 + 1)\omega_2\dot{q}_d - 2(\zeta_3 + 1)\omega_2^2q_d - \\ \quad \omega_2^3(\theta_d - \theta_{ref}), \\ \ddot{r}_d = -2(\zeta_4 + 1)\omega_3\dot{r}_d - 2(\zeta_4 + 1)\omega_3^2r_d - \\ \quad \omega_3^3\cos\theta(\psi_d - \psi_{ref}), \end{array} \right. \quad (27)$$

其中: ζ_i ($1 \leq i \leq 4$)为相对阻尼比, ω_i ($1 \leq i \leq 3$)为固有频率.

3.4 海流观测器设计(Ocean-current observer design)

令 u_{cn} , v_{cn} , w_{cn} 为惯性坐标系下海流速度, 根据运动学模型式(1)可得

$$\dot{\eta}_1 = R(\Theta)\nu_{1r} + V_{cn}, \quad (28)$$

其中: $V_{cn} = (u_{cn}, v_{cn}, w_{cn})^T \in \mathbb{R}^3$; \hat{V}_{cn} 表示 V_{cn} 的估计值, $\eta_1 = (x, y, z)^T \in \mathbb{R}^3$, $\hat{\eta}_1$ 表示 η_1 的估计值, $\nu_{1r} = (u - u_c, v - v_c, w - w_c)^T$.

设计海流观测器为^[9]

$$\left\{ \begin{array}{l} \dot{\hat{V}}_{cn} = K_3(\eta_1 - \hat{\eta}_1), \\ \dot{\hat{\eta}}_1 = R(\Theta)\nu_{1r} + \hat{V}_{cn} + K_4(\eta_1 - \hat{\eta}_1). \end{array} \right. \quad (29)$$

由式(28)–(29)可得

$$\left[\begin{array}{c} \dot{\hat{V}}_{cn} \\ \dot{\hat{\eta}}_1 \end{array} \right] = \left[\begin{array}{cc} -K_3 & I \\ -K_4 & 0 \end{array} \right] \left[\begin{array}{c} \tilde{V}_{cn} \\ \tilde{\eta}_1 \end{array} \right], \quad (30)$$

其中: K_3 , K_4 为控制参数矩阵, 当系统(30)的特征方程的根为严格正实时, 估计误差 $\tilde{V}_{cn} = V_{cn} - \hat{V}_{cn}$ 和 $\tilde{\eta}_1 = \eta_1 - \hat{\eta}_1$ 是渐近指数稳定的.

定理1 假设期望路径光滑且满足 $\eta_{1d}, \dot{\eta}_{1d} \in L_\infty$, 且 $\Theta_d, \dot{\Theta}_d, \ddot{\Theta}_d \in L_\infty$, 如果控制输入为式(26), 参数估计律为式(25), 海流观测器为式(29), 那么跟踪误差(e_1, e_2, e_3)将最终趋于零; 式(31) V_1 中所有信号一致最终有界.

定理1的证明详见下面的稳定性分析.

4 稳定性分析(Stability analysis)

定义Lyapunov函数为

$$V_1 = \frac{1}{2}Z_1^T K_1 Z_1 + \frac{1}{2}Z_2^T M Z_2 + \frac{1}{2} \sum_{i=1}^3 \tilde{\Theta}_i^T \Gamma_i^{-1} \tilde{\Theta}_i + \tilde{X}_1^T P \tilde{X}_1, \quad (31)$$

其中: $K_1 = \text{diag}\{k_{11}, k_{12}\} > 0$ 为控制参数, $\Gamma_i = \text{diag}(\gamma_{ij})$, $\tilde{X}_1 = [\tilde{V}_{cn} \ \tilde{\eta}_1]^T$.

对上式两边求导, 代入式(20)–(21)(25)(29), 整理得

$$\dot{V}_1 = Z_1^T K_1 \dot{Z}_1 + Z_2^T M \dot{Z}_2 +$$

$$\sum_{i=1}^3 \tilde{\Theta}_i^T \Gamma_i^{-1} \dot{\tilde{\Theta}}_i + \tilde{X}_1^T P \tilde{X}_1 + \tilde{X}_1^T P \dot{\tilde{X}}_1.$$

记 $A = \begin{bmatrix} -K_3 & I \\ -K_4 & 0 \end{bmatrix}$,

$$\dot{V}_1 = -Z_1^T K_1 Z_1 - Z_2^T D Z_2 - Z_2^T C_{\text{RB}} Z_2 - Z_2^T C_A Z_2 + Z_2^T (H^T T_1^T K_1 Z_1 + \tau - g - D\alpha + DV_c - C_{\text{RB}}\alpha - C_A\alpha + C_A V_c - M\dot{\alpha}) + \sum_{i=1}^3 \tilde{\Theta}_i^T \Gamma_i^{-1} \dot{\tilde{\Theta}}_i + \tilde{X}_1^T A^T P \tilde{X}_1 + \tilde{X}_1^T P A \tilde{X}_1.$$

由式(3)知, $Z_2^T C_{\text{RB}} Z_2 = 0$, $Z_2^T C_A Z_2 = 0$.

结合式(26), 则存在正定矩阵 P , 使 $A^T P + PA = -Q$, Q 为赫米特矩阵, 使

$$\dot{V}_1 \leq -Z_1^T K_1 Z_1 - Z_2^T (D + K_2) Z_2 - \tilde{X}_1^T Q \tilde{X}_1 \leq -\lambda_{\min}(K_1) \|Z_1\|^2 - \lambda_{\min}(D + K_2) \|Z_2\|^2 - \frac{1}{2} \sum_{i=1}^3 \tilde{\Theta}_i^T \Gamma_i^{-1} \tilde{\Theta}_i + \frac{1}{2} \sum_{i=1}^3 \tilde{\Theta}_i^T \Gamma_i^{-1} \tilde{\Theta}_i - \lambda_{\min}(Q) \|\tilde{X}_1\|^2,$$

则

$$\dot{V}_1 \leq -\mu V_1 + \delta, \quad (32)$$

其中:

$$\alpha_1 = \varsigma_2 \|X_1^*(t_0)\|, \quad \sigma_1 = 0.5\mu, \quad \varsigma_1 = \sqrt{\frac{\delta}{\mu \min(0.5, 0.5\lambda_{\min}(M))}},$$

$$\varsigma_2 = \sqrt{\frac{\max(0.5, 0.5\lambda_{\min}(M), 0.5\gamma_{1j}^{-1}, 0.5\gamma_{2j}^{-1}, 0.5\gamma_{3j}^{-1}, \lambda_{\min}(P))}{\min(0.5, 0.5\lambda_{\min}(M), \lambda_{\min}(P))}}.$$

定义Lyapunov函数

$$V_2 = \frac{1}{2} e_1^2 + \frac{1}{2} e_2^2 + \frac{1}{2} e_3^2, \quad (36)$$

$$\dot{V}_2 = e_1 \dot{e}_1 + e_2 \dot{e}_2 + e_3 \dot{e}_3.$$

代入式(5)–(6), 可得

$$\dot{V}_2 = -\delta_1 e_1^2 + e_2 U \sin(\chi - \chi_p) \cos(v - v_p) - e_3 U \sin(v - v_p) = -\delta_1 e_1^2 + e_2 U \sin(z_{12} + \chi_R) \cos(z_{11} + v_R) - e_3 U \sin(z_{11} + v_R). \quad (37)$$

代入式(7)–(8), 整理得

$$\dot{V}_2 = -\delta_1 e_1^2 - \frac{\delta_2 U}{\sqrt{\Delta_2^2 + e_3^2}} (e_2^2 \cos z_{12} \cos z_{11} - e_2 \Delta_1 \sin z_{12} \cos z_{11}) - \frac{U}{\sqrt{\Delta_2^2 + e_3^2} \sqrt{\Delta_1^2 + e_2^2}} \cdot (e_2 e_3 \Delta_1 \sin z_{12} \sin z_{11} - e_2^2 e_3 \sin z_{11} \cos z_{12}) - \frac{U}{\sqrt{\Delta_2^2 + e_3^2}} (\Delta_2 e_3 \sin z_{11} + e_3^2 \cos z_{11}). \quad (38)$$

因为 $|u_d| \geq |u_{d,\min}| > 0$, 则存在有限时间 $t_1 \geq t_0 \geq 0$, 使 $U \geq U_{\min} > 0$, $\forall t \geq t_1$. 而且存在 $t_2 \geq t_1$,

$$K_2 = \text{diag}\{k_{21}, k_{22}, k_{23}, k_{24}, k_{25}, k_{26}\},$$

$$\mu = \min(1, 2\lambda_{\min}(K_1), \frac{2\lambda_{\min}(D + K_2)}{\lambda_{\max}(M)}, \frac{\lambda_{\min}(Q)}{\lambda_{\max}(P)}),$$

$$\delta = \frac{1}{2} \sum_{i=1}^3 \tilde{\Theta}_i^T \Gamma_i^{-1} \tilde{\Theta}_i, \quad V_1(t) \leq V_1(t_0) e^{-\mu(t-t_0)} + \frac{\delta}{\mu}. \quad (33)$$

进一步得到

$$\min\left(\frac{1}{2}, \frac{1}{2}\lambda_{\min}(M), \frac{1}{2}\gamma_{ij}^{-1}, \lambda_{\min}(P)\right) \|X(t)\|^2 \leq \|X^*(t_0)\| \max\left(\frac{1}{2}, \frac{1}{2}\lambda_{\min}(M), \frac{1}{2\gamma_{1j}}, \frac{1}{2\gamma_{2j}}, \frac{1}{2\gamma_{3j}}, \lambda_{\min}(P)\right) e^{-\mu(t-t_0)} + \frac{\delta}{\mu}, \quad (34)$$

其中: $X(t) = [Z_1 \ Z_2 \ \tilde{\Theta}_1 \ \tilde{\Theta}_2 \ \tilde{\Theta}_3 \ \tilde{X}_1]^T$, $X^*(t_0) = [Z_1(t_0) \ Z_2(t_0) \ \tilde{\Theta}_1^T(t_0) \ \tilde{\Theta}_2^T(t_0) \ \tilde{\Theta}_3^T(t_0) \ \tilde{X}_1(t_0)]^T$.

因此, 可知

$$\|X(t)\| \leq \alpha_1 e^{-\sigma_1(t-t_0)} + \varsigma_1, \quad (35)$$

其中:

使 $|z_1| \leq |z_{1,ss}|$, 其中: $\dot{V}_2(z_{1,ss}) < 0$, 定义在 (t_1, t_2) 区间上, $\dot{V}_2 \geq 0$. $(U, \cos z_{11}, \sin z_{11}, \sin z_{12}, \cos z_{12}) \in L_\infty$, 因此对从任意点出发的 $e_1(t_0), e_2(t_0), e_3(t_0)$, 当 $t \rightarrow \infty$, $(e_1, e_2, e_3) \rightarrow 0$.

5 仿真实验(Simulation validation)

仿真实验采用文献[13]中参数, 如表1所示, 考虑控制器中AUV模型参数未知, 对上述研究的三维路径跟随控制方法的正确性和有效性进行验证.

表 1 AUV模型参数

Table 1 AUV model parameters

$m = 185 \text{ kg}$	$Y_v = -100 \text{ kg/s}$
$I_x = 25 \text{ kg} \cdot \text{m}^2$	$Z_w = -100 \text{ kg/s}$
$I_y = 50 \text{ kg} \cdot \text{m}^2$	$K_p = -30 \text{ kg} \cdot \text{m}^2/\text{s}$
$I_z = 50 \text{ kg} \cdot \text{m}^2$	$M_q = -50 \text{ kg} \cdot \text{m}^2/\text{s}$
$X_{\dot{u}} = -30 \text{ kg}$	$N_r = -50 \text{ kg} \cdot \text{m}^2/\text{s}$
$X_{\dot{v}} = -80 \text{ kg}$	$X_u _u = -100 \text{ kg/m}$
$Z_{\dot{w}} = -80 \text{ kg}$	$Y_{v v } = -200 \text{ kg/m}$
$K_p = -15 \text{ kg} \cdot \text{m}^2$	$Z_{w w } = -200 \text{ kg/m}$
$M_q = -30 \text{ kg} \cdot \text{m}^2$	$K_{p p } = -50 \text{ kg} \cdot \text{m}^2$
$N_r = -30 \text{ kg} \cdot \text{m}^2$	$M_{q q } = -100 \text{ kg} \cdot \text{m}^2$
$X_u = -70 \text{ kg/s}$	$N_{r r } = -100 \text{ kg} \cdot \text{m}^2$

参考轨迹为

$$x_d = 10 \cos(s/15), y_d = 10 \sin(s/15), z_d = s.$$

各变量初值取:

$$(x(0), y(0), z(0), \varphi(0), \theta(0), \psi(0), u(0), v(0), w(0), p(0), q(0), r(0)) = (-10, 0, -5, 0, 0, 0, 0.5, 0, 0, 0, 0, 0, 0), \\ (\hat{x}(0), \hat{y}(0), \hat{z}(0), \hat{u}_{cn}(0), \hat{v}_{cn}(0), \hat{w}_{cn}(0)) = (0, 0, 0, 0, 0, 0).$$

模型参数估计的初值取为实际的0.7.

惯性坐标系下的海流为 $[0.3 \quad -0.2 \quad 0]^T$.

滤波器参数: $\zeta_1 = 0.6, \zeta_2 = 0.6, \zeta_3 = 0.5, \zeta_4 = 0.5, \omega_1 = 0.8, \omega_2 = 10, \omega_3 = 10$.

控制器参数: $K_1 = I^{2 \times 2}, K_2 = I^{6 \times 6}$, 其中: I 为单位阵; $\Delta_1 = 5, \delta_2 = 1, \delta_1 = 1, K_3 = I^{3 \times 3}, K_4 = I^{3 \times 3}$.

图2为AUV实际路径和期望路径的跟踪曲线, 由图可看出, 在模型中存在未知海流干扰和模型参数未知的情况下, 控制器可使欠驱动AUV较好地跟踪上期望轨迹。为清晰看出跟踪效果, 仿真了3个坐标轴下的跟踪误差, 见图3。图4~6分别为纵向速度、俯仰角、偏航角跟踪误差, 可以看出经过开始的10 s左右的振荡后, 误差收敛于零值附近的邻域内。图7和图8为观测器输出的惯性坐标系下海流速度和位置估计误差, 由于观测器子系统是指数稳定, 从图中可以看出估计效果较好。图9~11为反步法中的虚拟控制误差跟踪曲线, 可以看出控制器使误差一致最终有界。

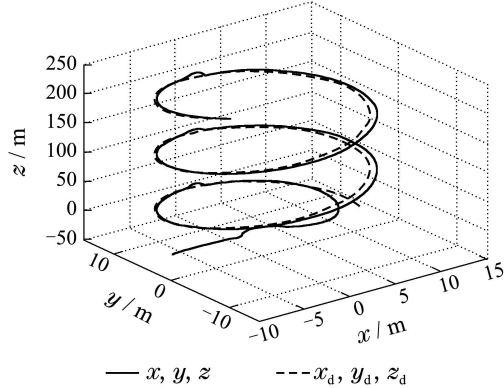


图2 AUV 三维路径跟踪曲线图

Fig. 2 Path following diagram of AUV in 3D

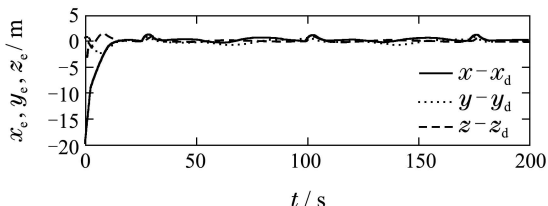


图3 x, y, z 路径误差

Fig. 3 Path errors x, y and z

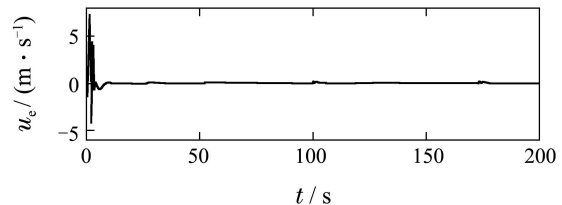


图4 纵向速度跟踪误差

Fig. 4 Surge velocity following error

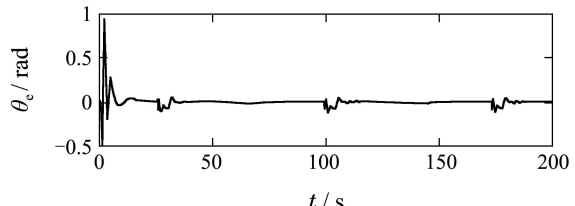


图5 倾仰角跟踪误差

Fig. 5 Pitch angle following error

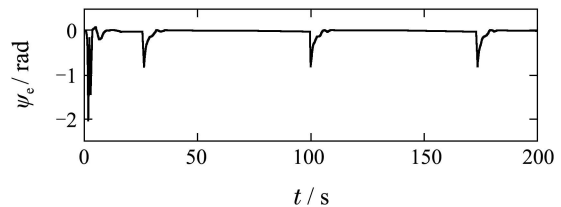


图6 偏航角跟踪误差

Fig. 6 Yaw angle following error

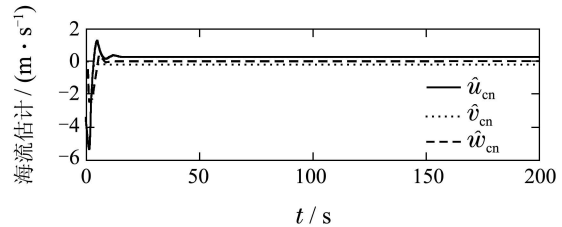


图7 海流速度估计误差

Fig. 7 Ocean current velocities estimation errors

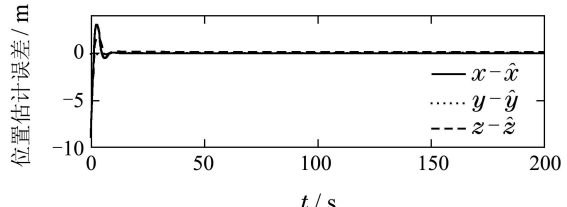


图8 位置估计误差

Fig. 8 Position estimation errors

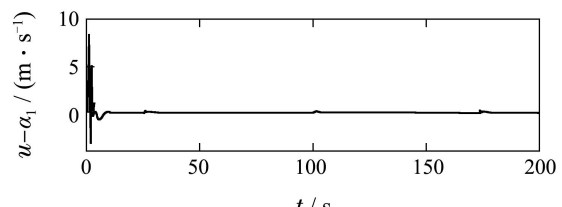
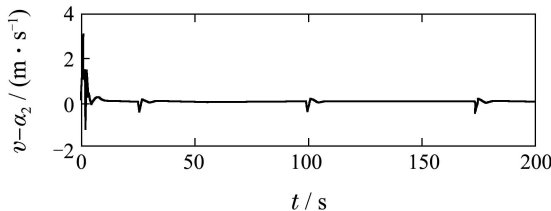
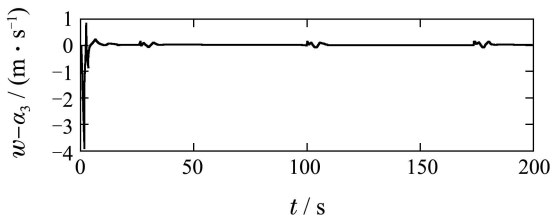


图9 z_{21} 跟踪误差

Fig. 9 z_{21} following error

图 10 z_{22} 跟踪误差Fig. 10 z_{22} following error图 11 z_{23} 跟踪误差Fig. 11 z_{23} following error

6 结论(Conclusions)

本文研究了存在未知海流干扰和模型参数未知情况下欠驱动AUV的三维路径跟随问题,提出了基于海流观测器的自适应控制器,利用死区方法估计未知模型参数,利用海流观测器估计AUV惯性坐标系下的海流速度和位置,减小了由于传感器噪声引起的测量误差。通过理论研究和仿真实验,可知本文提出的控制器能够克服常值海流干扰及模型参数未知的影响,具有较好的鲁棒性和很好的跟踪效果。

参考文献(References):

- [1] 王芳,万磊,李晔,等.欠驱动AUV的运动控制技术综述[J].中国造船,2010,51(2): 227–241。
(WANG Fang, WAN Lei, LI Ye, et al. A survey on development of motion control for underactuated AUV [J]. *Shipbuilding of China*, 2010, 51(2): 227–241.)
- [2] 贾鹤鸣,张利军,程相勤,等.基于非线性迭代滑模的欠驱动UUV三维航迹跟踪控制[J].自动化学报,2012,38(2): 308–314。
(JIA Heming, ZHANG Lijun, CHENG Xiangqin, et al. Three-dimensional path following control for an underactuated UUV based on nonlinear iterative sliding mode[J]. *Acta Automatica Sinica*, 2012, 38(2): 308–314.)

- [3] 俞建成,李强,张艾群,等.水下机器人的神经网络自适应控制[J].控制理论与应用,2008,25(1): 9–13。
(YU Jiancheng, LI Qiang, ZHANG Aiqun, et al. Neural network adaptive control for underwater vehicles [J]. *Control Theory & Applications*, 2008, 25(1): 9–13.)
- [4] DO K D, PAN J. *Control of Ships and Underwater Vehicles* [M]. London: Springer, 2009.
- [5] DO K D, JIANG Z P, PAN J, et al. A global output-feedback controller for stabilization and tracking of underactuated ODIN: A spherical underwater vehicle [J]. *Automatica*, 2004, 40(1): 117–124.
- [6] AGUIAR A P, PASCOAL A M. Dynamic positioning and way-point tracking of underactuated AUVs in the presence of ocean currents [C] //Proceedings of the 41st IEEE Conference on Decision and Control. Las Vegas, Nevada, USA: IEEE, 2002, 12: 2105–2110.
- [7] LAPIERRE L, SOETANTO D. Nonlinear path-following control of an AUV [J]. *Ocean Engineering*, 2007, 34(11/12): 1734–1744.
- [8] BREIVIK M, FOSSEN T I. A unified control concept for autonomous underwater vehicles [C] //Proceeding of the 2006 American Control Conference. Minneapolis, Minnesota, USA: IEEE, 2006, 6: 4920–4926.
- [9] ALONGE F, IPPOLITO F D, RAIMONDI F M. Trajectory tracking of underactuated underwater vehicles [C] //Proceeding of the 40th IEEE Conference on Decision and Control. Orlando, Florida, USA: IEEE, 2001, 12: 4421–4426.
- [10] REFSNES J E, SØRENSEN A J, PETTERSEN K Y. Model-based output feedback control of slender-body underactuated AUVs: theory and experiments [J]. *IEEE Transactions on Control Systems Technology*, 2008, 16(5): 930–946.
- [11] FOSSEN T I. *Marine Control Systems: Guidance, Navigation and Control of Ships, Rigs and Underwater Vehicles* [M]. Trondheim, Norway: Marine Cybernetics, 2002.
- [12] SLOTINE J E, LI W P. 应用非线性控制 [M]. 程代展,译. 北京: 机械工业出版社, 2006.
- [13] FJELLSTAD O E. *Control of unmanned underwater vehicles in six degrees of freedom a quaternion feedback approach* [D]. Norway: the Norwegian Institute of Technology University of Trondheim, 1994.

作者简介:

杨莹 (1976–),女,博士研究生,研究方向为水下机器人的非线性控制, E-mail: yangying06@hrbeu.edu.cn;

夏国清 (1962–),男,教授,博士生导师,研究方向为潜器与水下机器人控制技术, E-mail: xiaguqing@hrbeu.edu.cn;

赵为光 (1972–),男,博士研究生,研究方向为船舶及蒸汽动力装置建模与控制, E-mail: zhaoweiguang@hrbeu.edu.cn.